

Synthesis and structural and magnetic characterisation of tetranuclear Cu(II) complexes possessing novel $[\text{Cu}_4(\mu_4\text{-PO}_4)_2(\mu_2\text{-CO}_3)]$ butterfly cores that exhibit supramolecular isomerism[†]

Robert P. Doyle,^{‡a} Paul E. Kruger,^{*a} Boujemaa Moubaraki,^b Keith S. Murray^b and Mark Nieuwenhuyzen^c

^a Department of Chemistry, Trinity College, Dublin 2, Ireland. E-mail: paul.kruger@tcd.ie

^b School of Chemistry, Monash University, PO Box 23, Clayton, Victoria 3800, Australia

^c School of Chemistry, The Queen's University of Belfast, Belfast, UK BT9 5AG

Received 5th August 2003, Accepted 4th September 2003

First published as an Advance Article on the web 17th September 2003

The reaction in water of $\text{Cu}(\text{OH})_2$ with 2,2'-bipyridine (bipy) and $(\text{NH}_4)_2\text{HPO}_4$ (4 : 4 : 2) in air leads to the formation of two structurally related complexes following the fixation of CO_2 : $\{[(\text{H}_2\text{O})_2\text{Cu}_4(\text{bipy})_4(\mu_4\text{-PO}_4)_2(\mu_2\text{-CO}_3)] \cdot 22.5\text{H}_2\text{O}\}$, **1**, and $\{[(\text{H}_2\text{O})_2\text{Cu}_4(\text{bipy})_4(\mu_4\text{-PO}_4)_2(\mu_2\text{-CO}_3)] \cdot 15.5\text{H}_2\text{O}\}$, **1a**, as determined by single crystal X-ray diffraction. Whilst each complex contains isostructural tetranuclear Cu(II) butterfly cores, they differ in the way they pack in the solid state: adjacent units in **1** align in parallel fashion, whereas those in **1a** form H-bonded dimers in an antiparallel arrangement. **1** and **1a** are therefore supramolecular isomers. **1** is encapsulated within an 'ice-like' 3D H-bonded water network whereas the solvent sheath about **1a** forms a 2D H-bonded network. A similar product results when bipy is replaced with 1,10-phenanthroline (phen) giving $\{[(\text{H}_2\text{O})_2\text{Cu}_4(\text{phen})_4(\mu_4\text{-PO}_4)_2(\mu_2\text{-CO}_3)] \cdot 21.5\text{H}_2\text{O}\}$, **2**, which possesses an isostructural butterfly core shrouded within a 3D H-bonded water network. **2** packs in the solid-state in a similar way to **1** although, in this instance, adjacent units align in an antiparallel fashion. Both **1** and **2** may be directly synthesised in higher yields when $(\text{NH}_4)\text{HCO}_3$ is included within the reaction medium. A magnetic susceptibility study performed upon **1** reveals net weak intramolecular antiferromagnetic coupling between the Cu(II) centres.

Introduction

There is considerable current interest in the synthesis of multinuclear transition metal complexes, with inspiration drawn from such disparate fields as bioinorganic and materials chemistry.¹ In particular, much attention has been given to copper because of the central role it plays in biology as an oxygen transport protein (dinuclear hemocyanin),² in the management of reactive oxygen intermediates (dinuclear superoxide dismutase)³ and as a redox catalyst affecting transformations of small molecules such as N_2O (tetranuclear nitrous oxide reductase)⁴ and O_2 (the trinuclear oxidases).⁵ Considerable effort has been given to the synthesis of multicopper complexes that serve as spectroscopic, structural and functional mimics of the active sites of these proteins.⁶ Multicopper compounds have also been extensively studied from a magneto-structural point-of-view due to the inherent interest of relating structure to magnetic exchange effects. Historically these are the best-understood systems.⁷

Our interests lie in the formation of multicopper complexes from both a bioinorganic modelling approach⁸ and from a quest to develop interesting magnetic materials with potentially high spin ground states.⁹ We have recently been attracted to the use of polyoxoanions of group 15 (P and As) in the synthesis of molecular coordination compounds.¹⁰ This is not only due to their biological significance, as metal ions are heavily involved in phosphate metabolism, but also to their potential role as mediators of magnetic exchange interactions. Hendrickson and co-workers have proposed that tetrahedrally disposed oxoanions of group 15 should propagate ferromagnetic coupling between Cu(II) centres.¹¹ Here, we report the synthesis and

structural and magnetic characterisation of Cu(II) compounds which possess novel tetranuclear butterfly cores: $[\text{Cu}_4(\mu_4\text{-PO}_4)_2(\mu_2\text{-CO}_3)]$. These species are readily prepared by simply mixing under air in aqueous solution: $\text{Cu}(\text{OH})_2$ and ammonium hydrogencarbonate with either 2,2'-bipyridine to give **1** and **1a**, or 1,10-phenanthroline to give **2**. The bridging carbonate ligand arises following CO_2 fixation from the air. Whilst phosphate has been shown to form many coordination modes to transition metals, to the best of our knowledge, these are the first examples of discrete transition metal complexes featuring $\mu_4\text{-O}, \text{O}', \text{O}''$ - PO_4^{3-} bridging. Typically, μ_4 -phosphate is limited to the polyoxometallates, layered infinite sheets and involves each oxygen atom in coordination.¹² It is also evident that **1**, **1a** and **2** crystallise with a high degree of hydration, and that the water forms ornate multi-dimensional H-bonded networks about the complexes. The nature of these networks is also discussed.

Experimental

Materials and methods

Solvents and chemicals were of laboratory grade and were used as received. IR spectra were recorded as KBr pellets on a Perkin Elmer Paragon 1000 FT-IR spectrometer in the 4000–400 cm^{-1} region. Chemical analyses; C, H, N, P were performed at the Micro-analytical laboratories, University College Dublin, Ireland. Magnetic measurements at RT were performed using a Faraday balance which incorporated a Newport electromagnet fitted with Faraday-profile pole faces. Diamagnetic corrections for ligand susceptibilities were made using Pascal's constants. Variable-temperature magnetic susceptibility measurements (300–4.2 K) were performed on powdered samples at field strength of 1 T using a Quantum Design M.P.M.S. Squid magnetometer following previously reported procedures.^{9a}

Synthesis of $\{[(\text{H}_2\text{O})_2\text{Cu}_4(\text{bipy})_4(\mu_4\text{-PO}_4)_2(\mu_2\text{-CO}_3)] \cdot 22.5\text{H}_2\text{O}\}$
1. Copper hydroxide (1 g; 10.2 mmol) was suspended in 100 ml of distilled water. To this was added an aqueous suspension of

[†] Electronic supplementary information (ESI) available: Figs. S1–3: Selected views of the 3D H-bonded water networks encapsulating **1**, **1a** and **2** showing oxygen–oxygen close contacts. See <http://www.rsc.org/suppdata/dt/b3/b309275e/>

[‡] Current address: Department of Chemistry, Yale University, P.O. Box 208107, New Haven, CT, 06520-8107, USA.

Table 1 Crystal data for **1**, **1a** and **2**

Compound	1	1a	2
Chemical formula	Cu ₄ C ₄₁ H ₃₂ N ₈ P ₂ O ₁₁ ·22.5H ₂ O	Cu ₄ C ₄₁ H ₃₂ N ₈ P ₂ O ₁₁ ·15.5H ₂ O	Cu ₄ C ₄₉ H ₃₂ N ₈ P ₂ O ₁₁ ·21.5H ₂ O
Formula weight	1521.53	1408.09	1612.27
Crystal system	Orthorhombic	Monoclinic	Triclinic
Space group	<i>Pnma</i>	<i>P2/c</i>	<i>P</i> $\bar{1}$
$\mu(\text{Mo-K}\alpha)/\text{mm}^{-1}$	1.107	1.658	1.421
<i>a</i> /Å	14.871(3)	14.250(9)	12.481(2)
<i>b</i> /Å	22.146(4)	18.49(1)	14.714(2)
<i>c</i> /Å	19.937(4)	21.40(1)	20.655(3)
α°	90	90	98.00(1)
β°	90	99.30(2)	100.84(1)
γ°	90	90	114.49(1)
<i>V</i> /Å ³	6566(2)	5564(6)	3288.8(8)
<i>Z</i>	4	4	2
<i>D_c</i> /g cm ⁻³	1.497	1.681	1.628
<i>T</i> /K	293(2)	153(2)	153(2)
$2\theta_{\text{max}}^\circ$	55.02	50.0	50.0
Min./max. trans. factor	0.806/1.000	0.6188/0.7326	0.8070/0.9452
<i>R</i> _{int}	0.1000	0.1341	0.0221
<i>R</i> ₁ , <i>wR</i> ₂ [<i>I</i> > 2σ(<i>I</i>)] ^a	0.0526, 0.1377	0.0789, 0.2002	0.0748, 0.1866
<i>R</i> ₁ , <i>wR</i> ₂ (all data)	0.1204, 0.1522	0.1356, 0.2352	0.1104, 0.2114
Reflections: collected, unique, observed	58321, 7205, 3705	39187, 9811, 5812	11941, 11366, 7933

$$^a R_1 = \sum ||F_o| - |F_c|| / \sum |F_o|, wR_2 = [\sum w(F_o^2 - F_c^2)^2 / \sum w(F_o^2)]^{1/2}.$$

2,2'-bipyridine (1.59 g; 10.2 mmol), followed within 5 min and after the generation of a deep blue colour, by the addition of solid ammonium hydrogenphosphate (0.676 g; 5.12 mmol). A royal blue solution developed and was stirred over 72 h. After filtration, parallelepiped crystals grew by slow evaporation at ambient temperatures after several days. The extremely fragile crystals lost solvent rapidly on removal from their mother-liquor. Due to this instability a sample for analysis was dried *in vacuo* at 60 °C for 24 h to generate the anhydrous phase of **1**; 53% isolated yield. Found: C, 41.9; H, 3.5; N, 9.3; P, 5.1%. Cu₄C₄₁H₃₆N₈O₁₃P₂ requires: C, 42.27; H, 3.11; N, 9.62; P, 5.32%. IR (KBr): 3420vs br, 1654m, 1599m, 1561m, 1444w, 1316m, 1253w, 1103sh, 1061s, 1001s, 772m cm⁻¹. $\lambda_{\text{max}}/\text{nm}$ (H₂O): 687 (253 M⁻¹ cm⁻¹). μ_{eff} (295 K) = 1.78 μ_{B} .

Isolation of [(H₂O)₂Cu₄(bipy)₄(μ₄-PO₄)₂(μ₂-CO₃)]·15.5H₂O **1a.** When a solution of **1** was allowed to stand for a week or more, small blue block-like crystals also deposited. Whilst analytical data were similar to **1**, the crystal morphology suggested a different product, which was subsequently confirmed by a single crystal X-ray diffraction study. The crystals lost solvent rapidly following removal from their mother-liquor. Due to this instability a sample for analysis was dried *in vacuo* at 60 °C for 24 hrs to generate the anhydrous phase of **1a**; 20% isolated yield. Found: C, 42.1; H, 3.6; N, 9.4; P, 5.1%. Cu₄C₄₁H₃₆N₈O₁₃P₂ requires: C, 42.27; H, 3.11; N, 9.62; P, 5.32%. IR (KBr): 3425vs br, 1650m, 1600m, 1558m, 1448w, 1321m, 1108sh, 1058s, 999s, 768m cm⁻¹. $\lambda_{\text{max}}/\text{nm}$ (H₂O): 691 (248 M⁻¹ cm⁻¹). μ_{eff} (295 K) = 1.76 μ_{B} .

Synthesis of [(H₂O)₂Cu₄(phen)₄(μ₄-PO₄)₂(μ₂-CO₃)]·21.5H₂O **2.** A similar method to that used for the preparation of **1** was followed for the preparation of **2** by replacing 2,2'-bipyridine with 1,10-phenanthroline. A blue solution developed following the full dissolution of the ligand (~15 min) and was allowed to stir in air for 3 days. Blue diamond shaped crystals deposit on standing. The crystals slowly lost solvent on removal from their mother-liquor. Due to this instability a sample for analysis was dried *in vacuo* at 60 °C for 24 h to generate the anhydrous phase of **2**; 48% isolated yield. Found: C, 46.5; H, 3.1; N, 8.5; P, 4.7%. Cu₄C₄₉H₃₆N₈O₁₃P₂ requires: C, 46.67; H, 2.88; N, 8.89; P, 4.91%. IR (KBr): 3450br, 1640m, 1592m, 1520m, 1450m, 1333w, 1060sh, 1010w, 724s, 685w cm⁻¹. $\lambda_{\text{max}}/\text{nm}$ (H₂O): 685 (257 M⁻¹ cm⁻¹). μ_{eff} (295 K) = 1.80 μ_{B} .

Direct synthesis of **1 and **2** in the presence of (NH₄)HCO₃.** Copper hydroxide (0.5 g; 5.1 mmol) was suspended in 50 ml of distilled water. To this was added an aqueous suspension of 2,2'-bipyridine (0.795 g; 5.1 mmol) for **1** (or 1,10-phenanthroline (0.918 g; 5.1 mmol) for **2**) and ammonium hydrogencarbonate (0.1 g; 1.27 mmol) which immediately produced deep blue coloured solutions in each case. Solid ammonium hydrogenphosphate (0.388 g; 2.56 mmol) was added and the solutions evaporated over several days. Parallelepiped crystals of **1** and diamond shaped crystals of **2** deposit on standing in *ca.* 70% isolated yields. Spectroscopic data were consistent with those above and single crystal X-ray diffraction gave the same cell parameters.

Crystallographic measurements on **1**, **1a** and **2**

Crystal data and experimental details are summarised in Table 1. Single crystal analyses were performed at 168 K (**1**) and 153 K (**1a**) with a Bruker SMART CCD diffractometer using graphite monochromated Mo-Kα radiation ($\lambda = 0.71073$ Å). A full sphere of data was obtained for each using the omega/phi scan method. Data for (**2**) were collected at 153 K with a Siemens P4 diffractometer using graphite monochromated Mo-Kα radiation ($\lambda = 0.71073$ Å) using omega scans. Data were collected, processed, and corrected for Lorentz and polarization effects using XSCANS or SMART and SAINT-NT software.¹³ Absorption corrections were applied using SADABS (**1** and **1a**) and SHELXTL (**2**).¹³ The structures were solved using direct methods and refined with the SHELXTL program package. All non-hydrogen atoms were refined anisotropically. Aromatic hydrogen atoms were assigned to calculated positions using a riding model. Due to the high degree of hydration and disorder hydrogen atoms could not be located for the water molecules.

CCDC reference numbers 216728 (**1**), 216729 (**1a**) and 216730 (**2**).

See <http://www.rsc.org/suppdata/dt/b3/b309275e/> for crystallographic data in CIF or other electronic format.

Results and discussion

Synthesis and characterisation

We have reported previously the facile synthesis of the Cu(II) cluster, [Cu₆(bipy)₁₀(μ-CO₃)₂(μ-OH)₂](ClO₄)₆·4H₂O through

the reaction of an aqueous suspension of $\text{Cu}(\text{OH})_2$ with bipy in the presence of perchlorate as the precipitating anion.^{9a} In our current endeavour we wished to extend this methodology to incorporate other anions in place of perchlorate that may also act as ligand species. To this end we chose phosphate as it has potentially many varied coordinating modes, most typically as a bridging ligand.¹² In this regard, $\text{Cu}(\text{OH})_2$ and either bipy (**1**) or phen (**2**) were reacted in water in 1 : 1 stoichiometry to yield a turbid blue solution which clarified upon the addition of $(\text{NH}_4)_2\text{HPO}_4$. Slow evaporation of the resulting royal blue solutions yielded crystalline products of **1** and **1a** (as co-products) and **2** after several days. It should be noted that the abundance of **1a** as a proportion of the co-products increases as successive crops of **1** are removed from the mother-liquor and the longer that it is allowed to stand. Crystals of **1** are extremely fragile and easily shear when handled, whilst **1a** and **2** are mechanically more robust. Nevertheless, each loses solvent upon removal from their mother-liquors. Both **1** and **2** may be isolated more expediently and in higher yield when $(\text{NH}_4)\text{HCO}_3$ is incorporated directly into the reaction medium.

The infrared spectra of **1**, **1a** and **2** are grossly similar when allowance is made for the different coordinated ligands and contain two sharp absorption bands at *ca.* 1520 and 1320–1330 cm^{-1} , which are consistent with the presence of carbonate.¹⁴ The carbonate arose through the fixation of adventitious carbon dioxide within the aqueous solution, which is enhanced under the basic reaction conditions (pH *ca.* 10). Such a reaction is not without precedent for copper and other transition metal complexes.^{9a,15} The remainder of the infrared spectra are dominated by absorption bands from the bipy and phen ligands for **1**, **1a** and **2**, respectively, and by inorganic phosphate. The d–d spectra of aqueous solutions of each compound exhibit a very broad and featureless band centred at *ca.* 690 nm, which is consistent with the presence of a distorted square-pyramidal nature about each Cu(II) chromophore.¹⁶

Crystal structure of 1. The atomic numbering scheme and atom connectivity for **1** is shown in Fig. 1(a). As **1** is representative of the family a detailed description of the structure is given here, with any variation between it and **1a** and **2** highlighted when discussing them. The molecular structure of **1** is comprised of four slightly distorted square-pyramidal Cu(II) atoms in a parallelogram array, with a two-fold rotation axis about C(1s)–O(1s) relating each half of the molecule. Each Cu(II) is coordinated by a bipy ligand and linked by two μ_4 -phosphate groups. Further bridging between Cu(2) and Cu(2^a) ($a = x, \frac{1}{2} - y, \frac{1}{2} - z$) is furnished by carbonate, which is disordered over two sites about the two fold rotation axis. The N_2O_3 coordination chromophore about Cu(1) is provided by two bipy nitrogen donors and two phosphate oxygen atoms, which form the basal plane of the square-pyramid, with a bound water molecule occupying the apex of the pyramid. N_2O_3 coordination about Cu(2) is comprised of two bipy nitrogen donors, a phosphate oxygen O(11), with corner shared μ_2 -carbonate oxygen O(1s) completing the basal plane. Apical coordination is provided by the bridging phosphate oxygen O(13^a).

Bonding about each copper centre is as expected for square pyramidal geometry and varies with donor type and position with apical bond lengths significantly longer than the basal-plane ones, as might be anticipated by the Jahn–Teller theorem. Analysis of the shape determining angles using the approach of Reedijk and co-workers¹⁷ yields τ values of 0.160(1) for both Cu(1) and Cu(2) ($\tau = 0$ for perfect square pyramidal and 1 for trigonal bipyramidal geometries). Selected bond lengths and angles are contained within Table 2. Bonding about P(1) is consistent with the single and double bond nature of the coordinated and non-coordinated oxygen atoms, and whilst phosphate has been found to form numerous bridging interactions,¹² the mode exhibited here is unique amongst

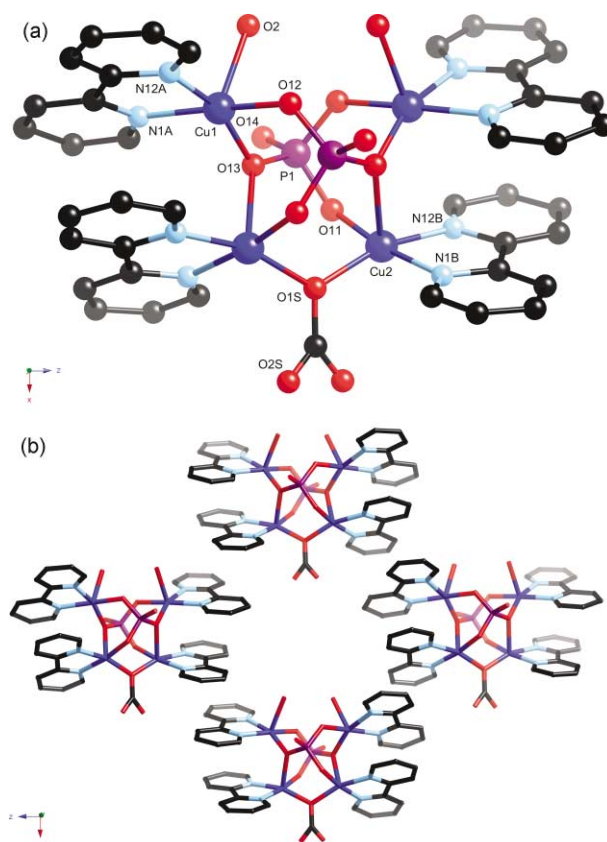


Fig. 1 (a) Molecular structure of **1** showing the butterfly core and atomic labelling scheme. (b) Packing diagram of **1** showing the 2D sheet formed by adjacent molecules. Note the parallel alignment of the molecules within the sheet; H-atoms and water of crystallisation omitted for clarity.

coordination compounds. This bridging mode disposes the four copper atoms in a butterfly arrangement with a $[\text{Cu}_4(\mu_4\text{-PO}_4)_2(\mu_2\text{-CO}_3)]$ core. Bridging between Cu(1) and Cu(2^a), through O(13) is asymmetric in nature [Cu(1)–O(13) 1.936(3) Å; Cu(2^a)–O(13) 2.413(3) Å], reflecting basal *vs.* axial disposition at Cu(1) and Cu(2^a), respectively, and subtends an angle of 96.4(1)°.

The positioning of the bipy ligands facilitates intramolecular offset π – π interactions with a dihedral angle between rings of $\sim 4^\circ$ and a separation at closest contact of 3.36 Å. This interaction supports the shortest Cu \cdots Cu distance of 3.259(7) Å between Cu(1) \cdots Cu(2^a). Other Cu \cdots Cu separations are greater, Table 2. The bipy ligands also participate in a continuous intermolecular π – π interaction along the crystallographic *x*-axis, with a dihedral angle between rings of $\sim 4^\circ$ and a separation at closest contact of 3.39 Å. This forms a 2D sheet in the *xz*-plane, Fig. 1(b). This association is also supported by an intermolecular H-bond between carbonate O(2s) and H(5^b) from an adjacent bipy ligand [C(5^b)–H(5^b) \cdots O(1s) 2.46 Å, 142.1°; $b = -\frac{1}{2} + x, +y, -z$]. All molecules within a given sheet align in a parallel manner, although adjacent molecules have opposite 'twist' *i.e.* the torsion angle between the mean planes containing the bipy ligands from across the butterfly core is *ca.* 47°. This twist places the Cu(1)-bound water within intramolecular H-bond distance to phosphate oxygen O(12) [O(2) \cdots O(12) 2.781(3) Å].¹⁸

The 2D sheets within the *xz*-plane contain 'cavities' within which some of the lattice water molecules reside. The potential solvent accessible area is 41.3% of the crystal.¹⁹ The combination of hydrophilic (PO_4^{3-} , CO_3^{2-} , bound H_2O) and hydrophobic (bipy π – π stack) regions in **1** has a dramatic effect upon the way that the lattice water molecules interact with it and with each other. The 2D sheets formed by the complex are separated by a layer of water, which probably accounts for relative ease of

Table 2 Selected bond lengths (Å) and angles (°) for **1**, **1a** and **2**

1	Cu(1)–O(13)	1.936(3)	Cu(2)–O(13 ^a)	2.413(3)
	Cu(1)–O(12)	1.938(3)	Cu(2)–O(11)	1.915(3)
	Cu(1)–O(2)	2.324(4)	Cu(2)–O(1s)	1.951(2)
	Cu(1)–Cu(1 ^a)	4.388(7)	Cu(1)–Cu(2)	5.011(7)
	Cu(1)–Cu(2 ^a)	3.259(7)	Cu(2)–Cu(2 ^a)	3.426(7)
	Cu(1)–O(13)–Cu(2 ^a)	96.4(1)	Cu(2)–O(1s)–Cu(2 ^a)	122.8(3)
1a	Cu(1)–O(11)	1.902(6)	Cu(2)–O(12)	1.941(6)
	Cu(1)–O(21)	1.931(6)	Cu(2)–O(22)	1.954(7)
	Cu(1)–O(1w)	2.343(7)	Cu(2)–O(2w)	2.309(6)
	Cu(3)–O(13)	1.912(7)	Cu(4)–O(23)	1.932(7)
	Cu(3)–O(31)	1.955(7)	Cu(4)–O(31)	1.953(7)
	Cu(3)–O(21)	2.302(7)	Cu(4)–O(12)	2.287(6)
	Cu(1)–Cu(2)	4.285(8)	Cu(2)–Cu(3)	4.954(8)
	Cu(1)–Cu(3)	3.248(8)	Cu(2)–Cu(4)	3.334(8)
	Cu(1)–Cu(4)	5.021(8)	Cu(3)–Cu(4)	3.343(7)
	Cu(1)–O(21)–Cu(3)	99.8(3)	Cu(2)–O(12)–Cu(4)	103.8(3)
	Cu(3)–O(31)–Cu(4)	117.6(3)		
	2	Cu(1)–O(11)	1.923(5)	Cu(2)–O(23)
Cu(1)–O(31)		1.944(5)	Cu(2)–O(1w)	2.274(5)
Cu(1)–O(23)		2.347(4)	Cu(2)–O(12)	1.938(6)
Cu(3)–O(13)		2.300(5)	Cu(4)–O(13)	1.953(5)
Cu(3)–O(31)		1.940(5)	Cu(4)–O(22)	1.911(5)
Cu(3)–O(21)		1.928(5)	Cu(4)–O(2w)	2.315(5)
Cu(1)–Cu(2)		3.238(7)	Cu(2)–Cu(3)	4.917(7)
Cu(1)–Cu(3)		3.360(7)	Cu(2)–Cu(4)	4.232(8)
Cu(1)–Cu(4)		4.999(8)	Cu(3)–Cu(4)	3.311(7)
Cu(1)–O(23)–Cu(2)		97.9(2)	Cu(3)–O(13)–Cu(4)	101.9(2)
Cu(1)–O(31)–Cu(3)		119.8(3)		

Symmetry code: a = $x, \frac{1}{2} - y, \frac{1}{2} - z$.

crystal shearing. The distinct hydrophilic regions within **1** result in the lattice waters more closely associating with them, through H-bonding to phosphate, carbonate and bound water molecules. The lattice water molecules are themselves involved in an intricate pattern of H-bonding with each other, forming a 3D array that encapsulates **1**, resulting in a pseudo-clathrate structure, Fig. 2 and Fig. S1 (ESI †). Aspects of the H-bonding are reminiscent of those found within ice and of water clusters proposed to occur within the liquid phase.²⁰ Recently, it has been shown that water can play a significant role in defining the molecular and supramolecular structures of coordination compounds.²¹

Crystal structure of 1a. The atomic numbering scheme and atom connectivity for **1a** is shown in Fig. 3(a). The structure of **1a** is very similar to **1** with four Cu(II) ions in slightly distorted square pyramidal geometry with each coordinated by a bipy ligand and bridged by μ_4 -inorganic phosphate and μ_2 -carbonate, forming an isostructural butterfly core. However, in contrast to **1** each Cu(II) centre in **1a** is crystallographically unique. Selected bond lengths and angles are contained within Table 2.

Whilst the structures of **1** and **1a** are grossly similar it is pertinent here to highlight the disparity between them, which ranges from relatively minor intramolecular differences in some bond lengths and angles within the tetranuclear cluster, to major discrepancies in the way the complexes associate with each other intermolecularly throughout the crystal lattice. Firstly, bonding about each Cu(II) centre is in accord with square pyramidal geometry and similarly suffer from Jahn–Teller distortion, although to a lesser degree than **1** (τ values of 0.080(1), 0.110(1), 0.230(1) and 0.195(1) for Cu(1) to Cu(4), respectively). This is more clearly demonstrated when considering the bond lengths between the Cu(II) centres to the bridging apical oxygen atoms. The Cu(3)–O(21) and Cu(4)–O(12) bond lengths of 2.302(7) and 2.287(6) Å, respectively, are significantly shorter than that observed in **1** (*cf.* Cu(2)–O(13) 2.413(3) Å). This compression is accompanied by an increase in the bond angle about the bridging oxygen atom [Cu(1)–O(21)–

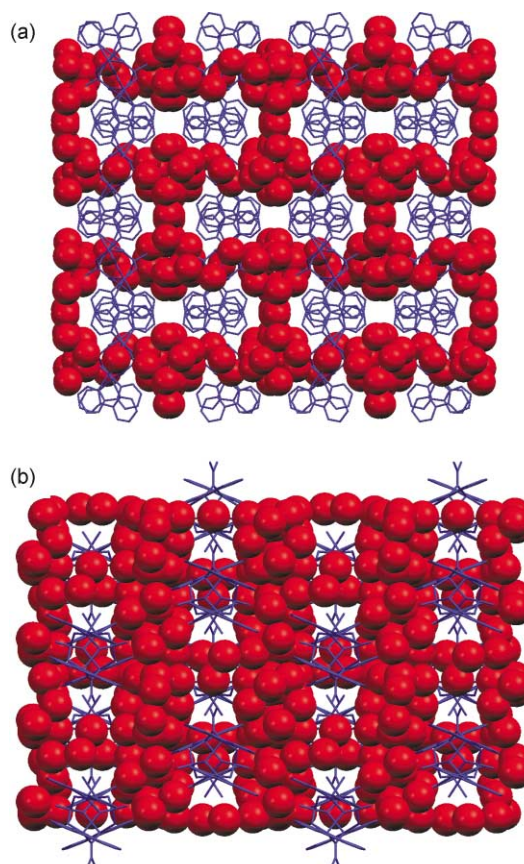


Fig. 2 Packing diagram of **1** with the water of crystallisation in space-filling mode to emphasise the oxygen–oxygen close contacts. (a) View down the crystallographic x -axis. (b) View down the crystallographic z -axis; H-atoms omitted for clarity.

Cu(3), 99.8(3)°; Cu(2)–O(12)–Cu(4), 103.8(3)° *cf.* Cu(1)–O(13)–Cu(2^a) 96.4(1)° for **1**], and results in a Cu(1) \cdots Cu(3) and Cu(2) \cdots Cu(4) separation of 3.248(8) and 3.334(8) Å,

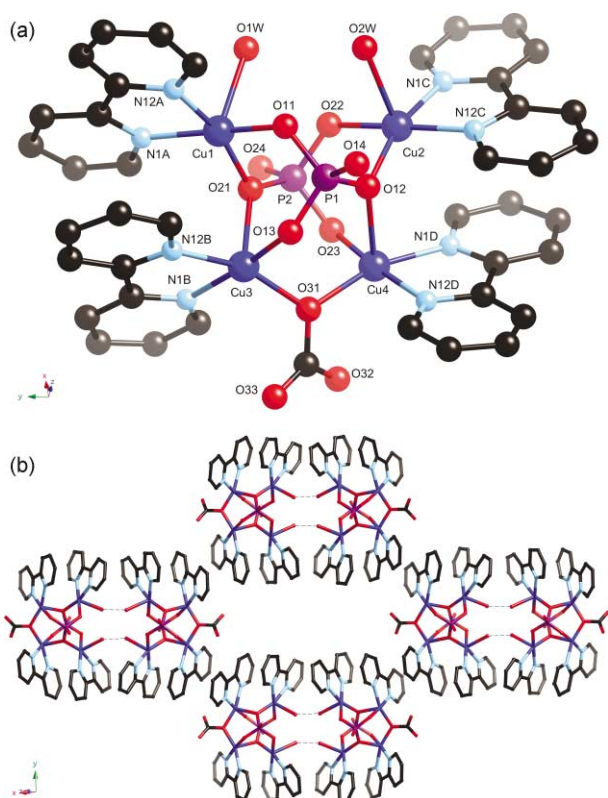


Fig. 3 (a) Molecular structure of **1a** showing the butterfly core and atomic labelling scheme. (b) Packing diagram of **1a** showing the 2D sheet formed by adjacent molecules. Note how adjacent molecules form H-bonded dimers in antiparallel alignment; H-atoms and water of crystallisation omitted for clarity.

respectively (*cf.* Cu(1) \cdots Cu(2^a) 3.259(7) Å for **1**). Furthermore, a contraction of the angle subtended about the carbonate bridge [Cu(3)–O(31)–Cu(4), 117.6(3)° *cf.* Cu(2)–O(1s)–Cu(2^a) 122.8(3)° for **1**] reduces the distance between these metal centres to 3.343(7) Å (*cf.* 3.426(7) Å in **1**). Other Cu \cdots Cu separations vary marginally and are given in Table 2. Additional bonding about the copper centres does not differ significantly from those found in **1**.

The bipy ligands participate in intramolecular offset π – π interactions with a dihedral angle between those coordinated to Cu(2) and Cu(4) of $\sim 6.5^\circ$ and a separation at closest contact of 3.28 Å. Those coordinated to Cu(1) and Cu(3) also participate in an offset π – π interaction with a separation at closest contact of 3.37 Å although, as the dihedral angle is $\sim 13.1^\circ$, this association is probably weaker. Furthermore, intermolecular π – π interaction occurs between those bipy ligands coordinated to Cu(3) and Cu(4) with their inversion related neighbours giving separation at closest contact of 3.37 and 3.53 Å, respectively, Fig. 3(b). This interaction is further supported by intermolecular H-bonding involving both carbonate oxygen atoms: O(33) with H(8^e) [C(8^e)–H(8^e) \cdots O(33) 2.49 Å, 135.5°; $c = 4 - x, -y, 2 - z$] and O(32) with H(5^d) [C(5^d)–H(5^d) \cdots O(32) 2.47 Å, 164.2°] and H(8^d) [C(8^d)–H(8^d) \cdots O(32) 2.26 Å, 164.4°; $d = 4 - x, -1 - y, 2 - z$] from adjacent bipy ligands. The torsion angles between the mean planes defined by the bipy ligands across the butterfly core are *ca.* 62°, indicating a more pronounced ‘twist’ compared to that found in **1**. This twist also places the bound water molecules O(1w) and O(2w) within an intramolecular H-bond distance of phosphate oxygen O(22) and O(11), respectively [O(1w) \cdots O(22) 2.77 Å; O(2w) \cdots O(11) 2.74 Å].¹⁸

The way the tetranuclear clusters pack throughout the crystal lattice is markedly different to that observed in **1**. Each cluster forms a dimer through intermolecular H-bonding between the apical water molecules, O(1w) and O(2w), with their symmetry equivalent neighbours on an adjacent cluster, [O(1w) \cdots

O(1w^e) 2.89 Å; O(2w) \cdots O(2w^e) 2.75 Å; $e = 3 - x, y, 1\frac{1}{2} - z$], Fig. 2(b). In essence the clusters buttress up against one another, which allows this H-bonding to occur and possibly accounts for the disruption in the π – π interactions noted above. These dimers pack together to form a 2D sheet in the ($\frac{1}{2} 0 -1$) plane, and create a ‘cavity’ of $\sim 1.4 \times 0.5$ nm within which lattice water molecules reside. This cavity is connected to others above and below the sheet to create channels running down the crystallographic x -axis, which are filled by water molecules within H-bond distance of each other. An additional channel runs between the sheets formed by the complex, although these are not fully occupied by water molecules and as such, the H-bonded water network only forms a 2D sheet within the crystallographic ac -plane, Fig. 4 (Fig. S2, ESI†). The potential solvent accessible area accounts for 26.7% of the crystal,¹⁹ which is markedly reduced from that of **1** (*cf.* 41.3%), and is consistent with the increased crystal density of **1a** with respect to **1**, 1.681 vs. 1.497 g cm^{–3}, respectively. This higher density would suggest **1a** is the thermodynamic product.

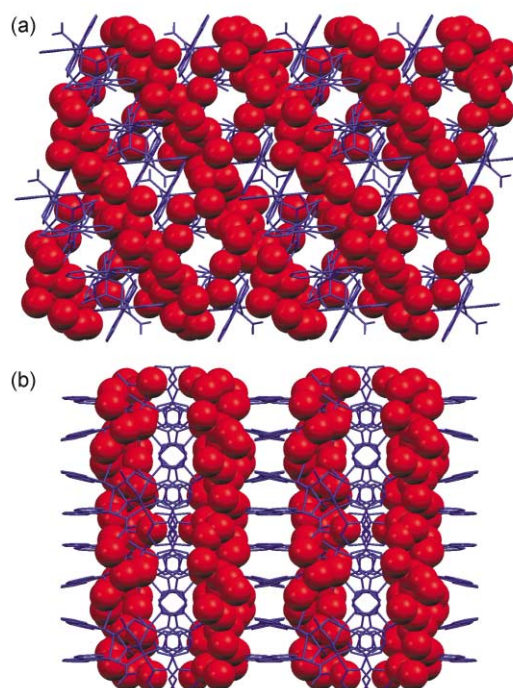


Fig. 4 Packing diagram of **1a** with the water of crystallisation in space-filling mode to emphasise the oxygen–oxygen close contacts. (a) View down the crystallographic y -axis. (b) View down the crystallographic z -axis; H-atoms omitted for clarity.

Crystal structure of 2. The atomic numbering scheme and atom connectivity for **2** is shown in Fig. 5(a). The molecular geometry of **2** is similar to **1a** with four crystallographically unique slightly distorted square-pyramidally disposed copper atoms (τ values of 0.190(1), 0.176(1), 0.160(1) and 0.183(1) for Cu(1) to Cu(4), respectively). In this instance phen ligands provide N₂ coordination about each copper. Bonding around each copper centre is indicative of Jahn–Teller distortion, with the axial bond-lengths closely resembling those found in **1a** *viz.* Cu(1)–O(23) 2.347(7) Å and Cu(3)–O(13) 2.300(5) Å, which are shorter than those found in **1** (*cf.* **1** Cu(2)–O(13^a) 2.413(3) Å and **1a** Cu(3)–O(21) 2.302(7) Å and Cu(4)–O(12) 2.287(6) Å). These minor changes affect the bridging angle between Cu(1) and Cu(2) through O(23), 97.9(1)°, and Cu(3) and Cu(4), 101.9(2)°, which are smaller than the comparable angles in **1a**, [99.8(3) and 103.8(3)°] although larger than that in **1** [96.4(1)°]. The bridging angle through carbonate, Cu(1)–O(31)–Cu(3) 119.8(3)°, lies mid-way between those for **1** and **1a**, respectively. The Cu \cdots Cu separations vary marginally from those found in **1** and **1a** and are given in Table 2.

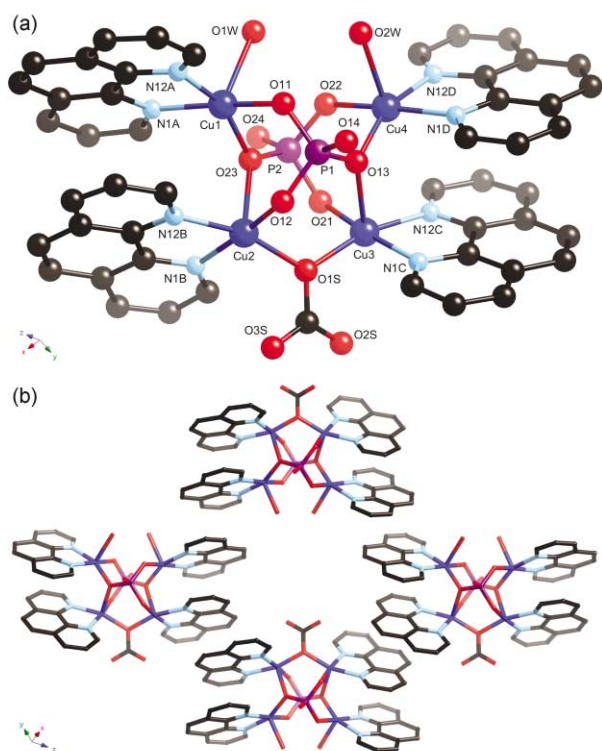


Fig. 5 (a) Molecular structure of **2** showing the butterfly core and atomic labelling scheme. (b) Packing diagram of **2** showing the 2D sheet formed by adjacent molecules. Note the antiparallel alignment of the molecules within the sheet; H-atoms and water of crystallisation omitted for clarity.

There are intramolecular offset π - π interactions between phen ligands with a dihedral angle between those coordinated to Cu(1) and Cu(2) of $\sim 7.0^\circ$ and a separation at closest contact of 3.20 Å. Those coordinated to Cu(3) and Cu(4) also participate in an offset π - π interaction with a separation at closest contact of 3.20 Å with a dihedral angle $\sim 5.2^\circ$. Furthermore, intermolecular π - π interactions occur between each phen ligand with their inversion related neighbours such that those coordinated to Cu(1), Cu(2), Cu(3) and Cu(4) give separations at closest contact of 3.34, 3.36, 3.33 and 3.28 Å, respectively, Fig. 5(b). This interaction is further supported by intermolecular H-bonding between both carbonate oxygen atoms: O(32) with H(6^f) [C(6^f)-H(6^f) \cdots O(32) 2.45 Å, 161.9° ; $f = -x, 2 - y, -z$] and O(33) with H(6^g) [C(6^g)-H(6^g) \cdots O(33) 2.56 Å, 159.7° ; $g = 1 - x, 2 - y, 1 - z$] from adjacent phen ligands. The torsion angles between the mean planes defined by the phen ligands across the butterfly core range from *ca.* 48 to 57° , indicating quite an uneven twist about the core which falls midway between those observed for **1** and **1a**. As before, the twist places the bound water molecules O(1w) and O(2w) within an intramolecular H-bond distance of phosphate oxygen O(22) and O(12), respectively [O(1w) \cdots O(22) 2.80 Å; O(2w) \cdots O(12) 2.75 Å].¹⁸

The way the tetranuclear clusters pack throughout the crystal lattice is reminiscent of, though fundamentally different to, that observed in **1**, and is markedly different to that found in **1a**, Fig. 5(b). Adjacent clusters are related by inversion and pack together to form a 2D sheet in the (-111) plane, with adjacent units in antiparallel alignment (*cf.* **1** where they are in parallel alignment). A $\sim 0.7 \times 0.5$ nm 'cavity' is contained within the sheet within which some H-bonded lattice water molecules reside. These cavities are further connected to others, above and below; through interaction with a 2D H-bonded water sheet that separates the 2D complex sheets. These H-bond interactions form a 3D water sheath that envelopes the complex, Fig. 6 (ESI, Fig S3†). The potential solvent accessible area accounts for 37.9% of the crystal,¹⁹ which is close to that of

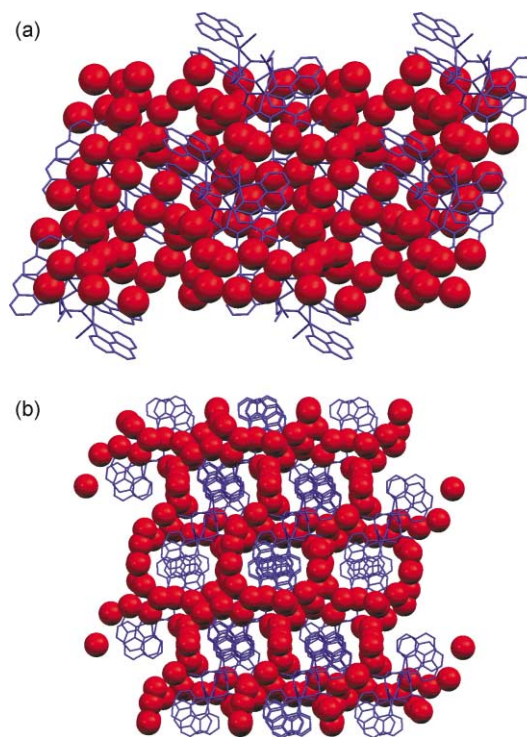


Fig. 6 Packing diagram of **2** with the water of crystallisation in space-filling mode to emphasise the oxygen-oxygen close contacts. (a) View down the crystallographic y -axis. (b) View down $(1-10)$; H-atoms omitted for clarity.

1 (*cf.* 41.3%), and an increase upon that found within **1a** (*cf.* 26.7%). In accord with the increased solvent accessible area, the crystal density of **2** (1.628 g cm^{-3}) is lower than **1** and **1a** (*cf.* 1.497 and 1.681 g cm^{-3} , respectively). We have not yet noted the appearance of any co-products (*i.e.* a putative '**2a**') with preparations involving phen.

Magnetic exchange in 1. To ascertain the existence, nature and degree of coupling between the Cu(II) centers, a variable temperature magnetic susceptibility study was carried out on powdered samples of **1** over the temperature range 4.2–300 K. Plots of χ_m vs. T (χ_m being the magnetic susceptibility per Cu(II) ion) and μ_{eff} vs. T are shown in Fig. 7. The resultant moment per copper decreases from $1.78 \mu_B$ to $0.70 \mu_B$ at 300 and 4.2 K, respectively. This behaviour is indicative of a very weak net antiferromagnetic interaction operating between the four copper centres. Clearly there are many magnetically viable exchange pathways in **1**, involving the bridge linkages that connect the equatorial Cu(II) magnetic lobes. Data fitting employed a two J model and considered only the coupling between Cu(1)–Cu(2a) and Cu(2)–Cu(2a) to be significant (others set to zero).²² An excellent fit was obtained with the following parameters: $J_{2,2a} = -9.5 \text{ cm}^{-1}$, $J_{1,2a} = -6.5 \text{ cm}^{-1}$, $g = 2.03$, $N_A = 64 \times 10^{-6} \text{ cm}^3 \text{ mol}^{-1}$ per Cu, with 0.1% 'monomer' impurity. Coupling between Cu(2) and Cu(2^a) through O(1s) is expected to be

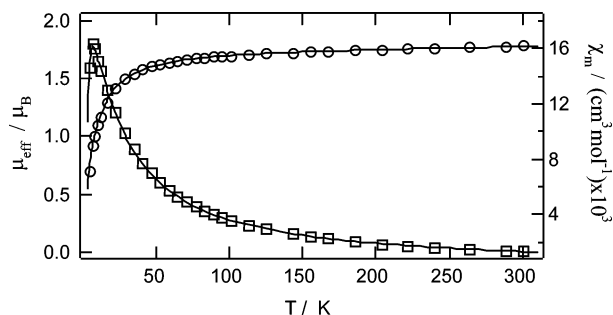


Fig. 7 The magnetic moment (○) and susceptibility (□) (per Cu) for **1** vs. temperature. The solid line is the calculated fit (see text).

dominant, although tilting of each 'magnetic plane' is evident (each half of the molecule is rotated by $\sim 47^\circ$ (*vide supra*) with respect to the other) and might be expected to attenuate any coupling. This may account for the weakness of the coupling found here. Furthermore, the Cu(1)–O(13)–Cu(2a) linkage involves an axial/equatorial orthogonal combination, so a ferromagnetic term might be anticipated, and this would further offset any antiferromagnetic term. In the light of these results and considering the similarity of the tetranuclear Cu(II) cores within the current family, variable temperature magnetic susceptibility studies were not performed upon either **1a** or **2**, as they might be anticipated to be very similar to **1**.

There are few quantitative studies of three-atom phosphato-bridged copper(II) compounds available for comparison. The work of Ainscough²³ suggests that such bridges should provide very small *J* values. A recent study by Ranford and co-workers²⁴ upon a dinuclear compound, $[\{\text{Cu}_2(\text{HL})(\text{H}_2\text{PO}_4)_2\}_2][\text{NO}_3]_2 \cdot 2\text{H}_2\text{O}$, where $\text{H}_2\text{L} = 2,2'$ -bis[1-(2-pyridyl)methylidene]thiocarbonylbis(hydrazine), which possessed a three-atom bridging $\text{H}_2\text{PO}_4^{2-}$ disposed in axial–equatorial positions with respect to adjacent copper(II) centers, gave a *J* value attributed to this bridging moiety of -16 cm^{-1} . We have also found similar strength weak antiferromagnetic coupling to be operative within Cu(II) dimers where bridging is furnished by $\mu_2\text{-H}_2\text{AsO}_4^-$.^{10b} In contrast, Spiccia *et al.*²⁵ found considerably stronger antiferromagnetic coupling through $\mu_3\text{-HPO}_4^-$ in $\{[\text{Cu}_3\text{L}(\mu\text{-OH})(\mu_3\text{-HPO}_4)(\text{H}_2\text{O})][\text{PF}_6]_3 \cdot 3\text{H}_2\text{O}\}_n$, where $\text{L} = 1,3,5\text{-tris}(1,4,7\text{-triazacyclonon-1-ylmethyl})\text{benzene}$, as in this instance the bridging interaction involved direct equatorial–equatorial linkages. Clearly, more work is needed to further delineate the factors contributing to the size and sign of any magnetic interaction through phosphate bridges.

Conclusion

We have shown a that a family of tetranuclear copper(II) complexes, $\{[(\text{H}_2\text{O})_2\text{Cu}_4(\text{bipy})_4(\mu_4\text{-PO}_4)_2(\mu_2\text{-CO}_3)] \cdot 22.5\text{H}_2\text{O}\}$ **1**, $\{[(\text{H}_2\text{O})_2\text{Cu}_4(\text{bipy})_4(\mu_4\text{-PO}_4)_2(\mu_2\text{-CO}_3)] \cdot 15.5\text{H}_2\text{O}\}$ **1a** and $\{[(\text{H}_2\text{O})_2\text{Cu}_4(\text{phen})_4(\mu_4\text{-PO}_4)_2(\mu_2\text{-CO}_3)] \cdot 21.5\text{H}_2\text{O}\}$ **2** may be readily prepared in water through the reaction of $\text{Cu}(\text{OH})_2$, a bidentate aromatic chelate (bipy or phen) and phosphate in the presence of a carbonate source. These complexes possess isostructural butterfly cores containing phosphate in a heretofore unprecedented $\mu_4\text{-O, O', O''-PO}_4^{3-}$ bridging mode. Whilst the complexes possess similar cores, the way that they pack throughout the crystal lattice varies such that **1** and **1a** form supramolecular isomers of each other (pseudo-polymorphs) with distinct crystal packing, whereas **2** displays a different packing mode again. Each crystallises with a high degree of hydration, and H-bonding between these generates pseudo-clathrate structures, enveloping each within ornate solvent sheaths of varying dimensionality. We are currently trying to ascertain whether further supramolecular isomers of this family might be crystallised in an effort to establish what factors lead to their preparation. We are also extending our synthetic approach to incorporate other transition metals and inorganic oxo-anions. The results from these studies will be reported in due course.

Acknowledgements

Funds from the Australian Research Council, Trinity College Academic Development Research fund and the Irish Higher Education Authorities Programme for Research in Third Level Institutions (PRTLII) supported this research. Similarly, the Trinity College Dean of Researcher's Academic Development Fund is gratefully acknowledged. We also thank Mr Brian Conerney for his assistance in generating some of the figures and Dr Anthea C. Lees for helpful discussion.

References and notes

- (a) G. J. Halder, C. J. Kepert, B. Moubaraki, K. S. Murray and J. D. Cashion, *Science*, 2002, **298**, 1762; (b) D. E. Fenton, *Chem. Soc. Rev.*, 1999, **28**, 159; (c) R. H. Holm, P. Kennepohl and E. I. Solomon, *Chem. Rev.*, 1996, **96**, 2239; (d) K. S. Murray, *Adv. Inorg. Chem.*, 1995, **43**, 261; (e) R. E. P. Wimpenny, *J. Chem. Soc., Dalton Trans.*, 2002, 1; (f) W. Wernsdorfer, N. Allaga-Alcalde, D. N. Hendrickson and G. Christou, *Nature*, 2002, **416**, 406; (g) S. Bhaduri, M. Pink and G. Christou, *Chem. Commun.*, 2002, 2352; (h) P. E. Kruger and V. McKee, *Chem. Commun.*, 1997, 1341; (i) P. E. Kruger, F. Launay and V. McKee, *Chem. Commun.*, 1999, 639.
- (a) E. I. Solomon, F. Tuzcek, D. E. Root and C. A. Brown, *Chem. Rev.*, 1994, **94**, 827; (b) C. Gerdemann, C. Eicken and B. Krebs, *Acc. Chem. Res.*, 2002, **35**, 183; (c) R. J. M. K. Gebbink, A. J. Sandee, F. G. A. Peters, S. J. van der Gaast, M. C. Feiters and R. J. M. Nolte, *J. Chem. Soc., Dalton Trans.*, 2001, 3056.
- I. Bertini, S. Mangani and M. S. Viezzoli, *Adv. Inorg. Chem.*, 1998, **45**, 127.
- K. Brown, M. Tegoni, M. Prudencio, A. S. Pereira, S. Besson, J. J. Moura, I. Moura and C. Cambillau, *Nat. Struct. Biol.*, 2000, **7**, 191.
- Multi-copper Oxidases*, ed. A. Messerschmidt, World Scientific, Singapore, 1997.
- (a) W. B. Tolman, *Acc. Chem. Res.*, 1997, **30**, 227; (b) T. D. P. Stack, *Dalton Trans.*, 2003, 1881; (c) T. Kruse, T. Weyhermuller and K. Wieghardt, *Inorg. Chim. Acta.*, 2002, **331**, 81; (d) P. Chaudhuri, M. Hess, T. Weyhermuller and K. Wieghardt, *Angew. Chem., Int. Ed.*, 1999, **38**, 1095; (e) W. Kaim, *Dalton Trans.*, 2003, 761.
- (a) *Magneto-Structural Correlations in Exchange Coupled Systems*, ed. R. D. Willett, D. Gatteschi and O. Kahn, NATO ASI Series, Ser. C, vol. 140, Reidel, Dordrecht, 1985; (b) W. H. Crawford, H. W. Richardson, J. R. Wasson, D. J. Hodgson and W. E. Hatfield, *Inorg. Chem.*, 1976, **15**, 2107; (c) L. Merz and W. Haase, *J. Chem. Soc., Dalton Trans.*, 1980, 875; (d) M. Handa, N. Koga and S. Kida, *Bull. Chem. Soc. Jpn.*, 1988, **61**, 3853; (e) L. K. Thompson, S. K. Mandal, S. S. Tandon, J. N. Bridson and M. K. Park, *Inorg. Chem.*, 1996, **35**, 3117; (f) J. Lorösch, U. Quotschalla and W. Haase, *Inorg. Chim. Acta.*, 1987, **131**, 229.
- (a) P. E. Kruger, G. D. Fallon, B. Moubaraki and K. S. Murray, *J. Chem. Soc., Dalton Trans.*, 2000, 713; (b) P. E. Kruger, B. Moubaraki, K. S. Murray and E. R. T. Tiekink, *J. Chem. Soc., Dalton Trans.*, 1994, 1219; (c) P. E. Kruger, B. Moubaraki and K. S. Murray, *Polyhedron*, 1997, **16**, 2659; (d) P. E. Kruger, B. Moubaraki and K. S. Murray, *J. Chem. Soc., Dalton Trans.*, 1996, 1223; (e) P. E. Kruger, B. Moubaraki and K. S. Murray, *J. Inorg. Biochem.*, 1995, **59**, 602; (f) P. E. Kruger, G. D. Fallon, B. Moubaraki and K. S. Murray, *J. Inorg. Biochem.*, 1993, **51**, 473; (g) P. E. Kruger, G. D. Fallon, B. Moubaraki and K. S. Murray, *J. Chem. Soc., Chem. Commun.*, 1992, 1726; (h) R. L. Elliot, P. Kruger, K. S. Murray and B. O. West, *Aust. J. Chem.*, 1992, **45**, 889.
- (a) P. E. Kruger, G. Fallon, B. Moubaraki, K. J. Berry and K. S. Murray, *Inorg. Chem.*, 1995, **34**, 4808; (b) R. J. Parker, K. D. Lu, S. R. Batten, B. Moubaraki, K. S. Murray, L. Spiccia, J. D. Cashion A. D. Rae and A. C. Willis, *J. Chem. Soc., Dalton Trans.*, 2002, 3723; (c) Tynan, P. Jensen, P. E. Kruger, A. C. Lees and M. Nieuwenhuyzen, *Dalton Trans.*, 2003, 1223.
- (a) R. P. Doyle, P. E. Kruger, M. Julve, F. Lloret and M. Nieuwenhuyzen, *Inorg. Chem.*, 2001, **40**, 1726; (b) R. P. Doyle, P. E. Kruger, M. Julve, F. Lloret and M. Nieuwenhuyzen, *CrystEngComm*, 2002, **4**, 13.
- S. L. Lambert, T. R. Felthouse and D. N. Hendrickson, *Inorg. Chim. Acta.*, 1978, **29**, L223.
- (a) R. C. Finn, J. Zubieta and R. C. Haushalter, *Prog. Inorg. Chem.*, 2003, **51**, 421; (b) N. Hamanaka and H. Imoto, *Inorg. Chem.*, 1998, **22**, 5844; (c) R. L. Paul, A. J. Amoroso, P. L. Jones, S. M. Couchman, Z. R. Reeves, L. H. Rees, J. C. Jeffery, J. A. McCleverty and M. D. Ward, *J. Chem. Soc., Dalton Trans.*, 1999, 1563; (d) Cambridge Structural Database, Version 5.23, April 2002.
- SAINT-NT, program for data collection and data reduction, Bruker-AXS, Madison, WI, 1998; G. M. Sheldrick, SHELXTL Version 5.0, A System for Structure Solution and Refinement, Bruker-AXS, Madison, WI, 1998.
- Infrared and Raman Spectra of Inorganic and Coordination Compounds*, Part B, ed. K. Nakamoto, John Wiley, New York, 1997.
- (a) G. A. van Albada, I. Mutikainen, O. S. Roubreau, U. Turpeinen and J. Reedijk, *Eur. J. Inorg. Chem.*, 2000, 2179; (b) M. Rodriguez, A. Llobet, M. Corbella, P. Muller, M. A. Uson, A. E. Martell and J. Reibenspies, *J. Chem. Soc., Dalton Trans.*, 2002, 2900; (c) H. Adams, D. Bradshaw and D. E. Fenton, *J. Chem. Soc.*,

- Dalton Trans.*, 2001, 3407; (d) M. Fondo, A. M. Garcia-Deibe, M. R. Bermejo, J. Sanmartin and A. L. Llamas-Saiz, *J. Chem. Soc., Dalton Trans.*, 2002, 4746.
- 16 A. B. P. Lever, *Inorganic Electronic Spectroscopy*, Elsevier, Amsterdam, 1968, p. 359.
- 17 A. W. Addison, T. Rao, J. Reedijk, J. van Rijn and G. C. Verschoor, *J. Chem. Soc., Dalton Trans.*, 1984, 1349.
- 18 Due to the high degree of hydration, thermal motion, disorder and partial occupancy associated with the water molecules hydrogen atoms could not be located. 'Hydrogen'-bonding was inferred by considering the O...O close contacts of water molecules involved.
- 19 A. L. Spek, PLATON – A Multipurpose Crystallographic Tool, Utrecht University, Netherlands 2000; Mercury 1.1, CCDC 2002.
- 20 (a) P. Ball, *H₂O: A Biography of Water*, Weidenfeld and Nicolson, London, 1999; (b) R. Ludwig, *Angew. Chem., Int. Ed.*, 2001, **40**, 1809.
- 21 (a) L. J. Barbour, G. W. Orr and J. L. Atwood, *Nature*, 1998, **393**, 671; (b) R. J. Doedens, E. Yohanes and M. I. Kahn, *Chem. Commun.*, 2002, 62; (c) S. Pal, N. B. Sankaran and A. Samanta, *Angew. Chem., Int. Ed.*, 2003, **42**, 1741; (d) K. Raghuraman, K. K. Katti, L. J. Barbour, N. Pillarsetty, C. L. Barnes and K. V. Katti, *J. Am. Chem. Soc.*, 2003, **125**, 6955; (e) R. J. Doedens, E. Yohannes and M. I. Khan, *Chem. Commun.*, 2002, 62; (f) J. N. Moorthy, R. Natarajan and P. Venugopalan, *Angew. Chem., Int. Ed.*, 2002, **41**, 3417; (g) S. Manikumari, V. Shivaiah and K. S. Das, *Inorg. Chem.*, 2002, **41**, 6953.
- 22 W. E. Hatfield and G. W. Inman, *Inorg. Chem.*, 1969, **8**, 1376.
- 23 E. W. Ainscough, A. M. Brodie, J. D. Ranford and J. M. Waters, *J. Chem. Soc., Dalton Trans.*, 1997, 1251.
- 25 L. Spiccia, B. Graham, M. T. W. Hearn, G. Lazarev, B. Moubaraki, K. S. Murray and E. R. T. Tiekink, *J. Chem. Soc., Dalton Trans.*, 1997, 4089.
- 24 B. Moubaraki, K. S. Murray, J. D. Ranford, X. Wang and Y. Xu, *Chem. Commun.*, 1998, 353.